The Manganese-Stabilizing Protein of Photosystem II Modifies the *in Vivo* Deactivation and Photoactivation Kinetics of the H_2O Oxidation Complex in *Synechocystis* sp. PCC6803[†]

Robert L. Burnap,* Ming Qian, and Coy Pierce

Department of Microbiology and Molecular Genetics, Oklahoma State University, Stillwater, Oklahoma 74078

Received August 18, 1995; Revised Manuscript Received November 13, 1995[⊗]

ABSTRACT: Dark deactivation and photoactivation of H_2O-splitting activity were examined in a directed mutant (ΔpsbO) of *Synechocystis* sp. PCC6803 lacking the extrinsic manganese-stabilizing protein of the photosystem II (PSII) reaction center complex. Rapid ($t_{1/2}$ = 10 min) losses of H_2O-splitting activity were observed for ΔpsbO cells kept in the dark, but not for wild-type cells. The loss of H_2O-splitting activity by ΔpsbO cells was suppressed by maintaining the cells under illumination and dark losses were rapidly ($t_{1/2}$ < 1 min) reversed by light. Photoactivation kinetics of ΔpsbO and wild-type cells were compared following hydroxylamine extraction of PSII Mn. Photoactivation of ΔpsbO cells under continuous illumination occurs at an intrinsically faster rate (about 4-fold) than the wild-type. Virtually all of the increase in the rate of photoactivation can be accounted for by a corresponding 4-fold increase in the relative quantum yield of photoactivation as indicated by the yield of photoactivation as a function of flash number. The flash frequency dependence of photoactivation indicates a multi-quantum process in the mutant resembling the wild-type, but with significant increases in yields at all flash frequencies examined. The higher quantum yield of photoactivation in ΔpsbO cells occurs in the absence of large changes in the kinetics of the rate-limiting dark rearrangement. The results are consistent with increased accessibility (or affinity) and photooxidation of Mn^{2+} at one or both of the two binding sites involved in the initial stages of the photoactivation mechanism. In the context of previous results, it is proposed that MSP regulates the binding/photooxidation of the second Mn^{2+} of the photoligation sequence, but not the first.

Oxygenic photosynthesis depends upon a cluster of four manganese atoms associated with the catalytic site of H_2O oxidation of the photosystem II (PSII)[1] complex. The Mn cluster is involved in the charge accumulation process accompanying the four-electron decomposition of $2H_2O$. Absorption of a quantum generates the highly oxidizing Chl species, $P680^+$, which is capable of oxidizing the redox active tyrosine, Y_Z, of the D1 protein, which in turn is capable of extracting an electron from the H_2O oxidation complex. With each productive charge separation within the reaction center, the H_2O oxidation complex advances one step through a cycle of oxidation states designated S_0-S_4, with S_4 an unstable intermediate that decays to S_0, completing the decomposition of two molecules of H_2O and yielding O_2 in the process.

The Mn cluster appears to be sequestered within a region of the PSII complex formed by intrinsic and extrinsic proteins at the lumenal surface of the thylakoid membrane [for reviews on PSII see, Andersson and Akerland (1987), Babcock et al. (1989), Debus (1992), and Ghanotakis and Yocum (1990)]. The stable ligation of Mn within this region does not simply involve the diffusion and binding of Mn into the coordination environment provided by the active site protein(s). Instead, the formation of an enzymatically active complex additionally requires light and involves the photooxidation of the incoming Mn and the coordination of Ca^{2+}. The entire process, which involves several intermediates and at least two quanta of light, is termed photoactivation (Cheniae & Martin, 1972a,b; Miyao & Inoue, 1991; Miyao-Tokutomi & Inoue, 1992; Ono & Inoue, 1982; Tamura & Cheniae, 1986, 1987; Tamura et al., 1989). During photoactivation, the average state of oxidation of the Mn increases from Mn^{2+} to higher oxidation states ($Mn^{\geq 3+}$) found in the active complex. The oxidation of Mn during photoactivation is thought to occur via the same pathway as used during the H_2O oxidation process: electrons are extracted from Mn via Y_Z, to reduce the photooxidant $P680^+$ (Miller & Brudvig, 1990).

The coordination environment of the Mn cluster remains obscure, although several lines of evidence point to the intrinsic D1 polypeptide as providing amino acid ligands [reviewed in Debus (1992)]. The major PSII chlorophyll

[†] This work was supported by USDA-CRGO Grant 92-37306-7820 (to R.L.B.).

* Corresponding author. Fax: 405-744-6790. E-mail: burnap@vms.ucc.okstate.edu.

[⊗] Abstract published in *Advance ACS Abstracts,* January 1, 1996.

[1] Abbreviations: Chl, chlorophyll; DCBQ, 2,6-dichloro-*p*-benzoquinone; DCMU, 3-(3,4-dichlorophenyl)-1,1-dimethylurea, inhibits electron transport between Q_A and Q_B; HA, hydroxylamine (NH_2OH); Hepes, 4-(2-hydroxyethyl)-1-piperazineethanesulfonic acid; MSP, manganese-stabilizing protein, extrinsic 33 kDa PSII protein; potassium ferricyanide, $K_3Fe(CN)_6$; Q_A, primary plastoquinone electron acceptor; Q_B, secondary, exchangeable plastoquinone electron acceptor; P680, photooxidizable chlorophyll species acting as primary electron donor of the reaction center; PSII, photosystem II; *psbO*, gene encoding the manganese-stabilizing protein; S_n, oxidation states of the H_2O-splitting enzyme where *n* represents the number of stored oxidizing equivalents; VO_2, velocity of oxygen evolution; Y_Z, redox active tyrosine of the D1 protein acting as secondary electron donor of the reaction center.

0006-2960/96/0435-874$12.00/0

binding polypeptides CP47 and CP43, which have proximal light-harvesting functions, also appear to have important roles in forming the catalytic site of H_2O oxidation, although whether or not Mn ligands are provided by these subunits remains to be determined (Bricker, 1990). Similarly, other intrinsic polypeptides, including cyt b_{559}, have yet to be excluded as providing ligands to catalytically active Mn. Current evidence suggests that the extrinsic polypeptides, which include the closely associated Mn-stabilizing protein (MSP), do not provide ligands to Mn, but instead stabilize the active conformation of the H_2O oxidation complex and maintain high local concentrations of Ca^{2+} and Cl^-, essential cofactors of the H_2O-splitting reaction.

Of the extrinsic polypeptides, MSP appears to be the most important for maintaining the integrity of H_2O-splitting enzyme, insofar as its removal results in the most dramatic and least reversible alterations in structure and activity. Biochemical removal of MSP destabilizes the binding of two of the four Mn atoms of the H_2O oxidation complex, which thereby loses the ability to catalyze H_2O oxidation (Kuwabara et al., 1985). The labile pair of Mn atoms remains bound to the enzyme if the removal of MSP is accompanied by the addition of >150 mM Cl^-. H_2O-splitting activity persists under these conditions, although with impaired kinetics. In the absence of MSP, the S_2 oxidation state of the H_2O oxidation complex is more stable (Burnap et al., 1992; Mayes et al., 1991,; Miyao et al., 1987; Vass et al., 1987), and the S_3-[S_4]-S_0 transition is retarded (Burnap et al., 1992; Miyao et al., 1987). The absence of MSP also increases the Ca^{2+} requirement of the H_2O-splitting reaction (Bricker, 1992; Philbrick et al., 1991) and renders the active site Mn more accessible to exogenous reductants (Tamura et al., 1990). Recent genetic results provide evidence that MSP controls the affinity and/or accessibility of Mn to the high-affinity binding site of the H_2O oxidation complex and may interact with the COOH terminus of the D1 protein which probably provides ligands to active site Mn (Chu et al., 1994a).

The present work stems from the observation that the H_2O oxidation activity of a *Synechocystis* PCC6803 mutant lacking MSP (ΔpsbO) is maximal when cells are maintained in the light (Burnap et al., 1994), and may fluctuate drastically on a minutes time scale depending upon whether cells are incubated in the dark or light (Engels et al., 1994). Similar effects are observed for certain mutants having short deletions within the large lumenal loop of CP47 (Gleiter et al., 1994, 1995). The present study characterizes these activity changes and compares the kinetics of photoactivation of ΔpsbO mutant and wild-type cells treated with hydroxylamine to extract active site PSII Mn (Cheniae & Martin, 1972a). Interestingly, the apparent rate constant of photoactivation is increased approximately 4-fold in the absence of MSP, and this increase can be attributed to increases in the apparent overall quantum yield of photoactivation.

MATERIALS AND METHODS

Synechocystis sp. PCC6803 (wild-type) and ΔpsbO cells were routinely maintained in BG-11 medium supplemented with 5 mM glucose as described previously (Williams, 1988). The ΔpsbO strain lacks the entire coding region for the extrinsic Mn-stabilizing protein, and its construction and characterization have been detailed previously (Burnap & Sherman, 1991). Experimental wild-type and ΔpsbO cultures were propagated in 2.5 L capacity turbidostats at a steady-state cell density corresponding to about 8 μg mL^{-1} Chl under Cool White (General Electric) fluorescent illumination of approximately 40 μEinsteins m^{-2} s^{-1} at 30 °C. Cultures were aerated by bubbling with air enriched with 3% CO_2. Light intensity measurements were performed with a LiCor sensor (Lincoln, NE). For most experiments, approximately 200 mL of cells was pelleted at 25 °C at 6000*g* for 10 min. The cells were resuspended to a chlorophyll concentration of 200 μg mL^{-1} in HN buffer (10 mM Hepes, 30 mM NaCl, pH 7.1) supplemented with 1 mM $CaCl_2$ and 50 μM $MnCl_2$. The addition of $MnCl_2$ and $CaCl_2$ was found to improve the reproducibility of the photoactivation experiments (see below). The resuspended cells were allowed to reequilibrate by incubation in the light (15−20 μEinsteins m^{-2} s^{-1}) on a rotary shaker at room temperature for at least 15 min, but no longer than 60 min prior to being used in experiments. Due to the tendency of oxygen evolution activity mutant cells to deactivate in the dark, as described below, this reequilibration period was essential to establish maximal PSII activity. Maximal rates of O_2 evolution (VO_2) were determined polarographically at 30 °C using a Clark-type electrode. Samples were resuspended in HN buffer supplemented with 0.6 mM DCBQ and 1 mM potassium ferricyanide, and oxygen evolution was measured in response to saturating red (>620 nm) illumination.

Hydroxylamine (HA) extraction of PSII Mn and photoactivation of HA-extracted cells were performed essentially according to Cheniae and Martin (1972). HA extraction of PSII Mn involved incubation with 1 mM hydroxylamine (from freshly prepared and neutralized 0.5 M stock) in total darkness for 10 min with gentle agitation. The NH_2OH-treated cells were pelleted at 25 °C at 12000*g* for 5 min and then resuspended to 10-fold the original suspension volume in HN buffer supplemented with $MnCl_2$ and $CaCl_2$ as above. This step was repeated 4−5 times, and on the last wash, the cells were resuspended to 200 μg of Chl mL^{-1}. These extraction and wash procedures were done in nearly total darkness. All samples were kept on a shaker at 25 °C and 150 rpm throughout the duration of the experiment.

For photoactivation in continuous light, HA-extracted cells (4 mL at 200 μg mL^{-1}) were placed in loosely covered 50 mL Erlenmeyer flasks on a rotary shaker under continuous illumination provided by Cool White fluorescent lights (General Electric). The incident intensity at the flasks was adjusted to be in the range 15−65 μEinsteins m^{-2} s^{-1}, depending on the experiment. Fifty microliter aliquots were withdrawn at set time intervals for determination of the light-saturated rate of oxygen evolution in the presence of DCBQ as described above. Maximal activity for HA-extracted cells was defined as the light-saturated DCBQ-supported O_2 evolution rates obtained *after* gradual photoactivation. The gradual photoactivation was performed by placing an aliquot of the HA-extracted sample under weak illumination of about 10 μEinsteins m^{-2} s^{-1} for approximately 45 min. This procedure produced the highest recoveries (typically ≥85%) of the original preextracted activity from the HA-extracted samples (see legends of Figures 4−6).

For flash photoactivation experiments, the NH_2OH-treated cells, at a chlorophyll concentration between 6 and 12 μg/mL, were loaded into a 1.6 mL chamber of a water-jacketed, magnetically-stirred glass oxygen electrode apparatus. Cells were flashed using an EG&G xenon lamp receiving a 4.5 J

discharge from a 5 μF capacitor connected to an EG&G PS-302 power supply. Flashes were filtered with a Wratten no. 9 yellow filter. Flashes (5 μs FWHM) were focused via a lens into the sample chamber, and the transmitted light was reflected back through the sample chamber via a mirror placed opposite the flash lamp. Saturation of PSII centers by the applied flashes was assessed by measurements of flash O_2 yield (in fully reactivated samples), varying the flash intensity with neutral density filters and varying the cell density in the sample chamber. With our instrumentation, the flash intensities remain relatively constant and oversaturating when the dark interval is greater than 50 ms. At high frequencies, the flash intensity declines due to limitations on the recharge rate of the xenon lamp capacitor. For example, the flash intensities are about 55−70% normal at 100 Hz (dark interval =10 ms). This intensity is at the margin of saturation of samples under the described conditions, and this defined the instrumental limit for experiments investigating the frequency response of photoactivation. Immediately following the flash sequence, light-saturated oxygen evolution activity in the presence of DCBQ was measured as described above.

Flash O_2 yield measurements were performed using a bare platinum electrode that permits the centrifugal deposition of samples upon the electrode surface. Dark-incubated samples containing 6 μg of Chl in HN buffer were centrifuged in a removable electrode unit (metal surfaces were cleaned with powered $NaHCO_3$ between measurements) at 5000*g* for 5 min at 25 °C in a Sorvall HB4A swing-out rotor. Flash O_2 yields were measured using a circuit that sets the polarization of the electrode and amplifies the ampermeric signal during flash excitation of the sample. This was constructed according to the electronic design of Meunier and Popovic (1988). Polarization of the electrode (0.73 V) was initiated 10 s before the initiation of data acquisition, and the flash sequence was initiated 333 ms after that. The amplified electrode signal from this circuit was digitized by an analog to digital/digital to analog computer plug-in board (AT-MIO-16F, National Instruments, Austin, TX), which also controlled the timing of the polarization of the electrode, data acquisition, and the firing of the xenon actinic flashes.

RESULTS

O_2 evolution activity in the ΔpsbO mutant declines rapidly ($t_{1/2}$ = 18 min) when cells are incubated in the dark (Figure 1). The decay of activity in dark ΔpsbO cells was significantly accelerated ($t_{1/2}$ = 10 min) by the presence of glucose in the incubation medium at concentrations typically utilized to support photoheterotrophic growth in *Synechocystis*. Although the basis of the glucose effect was not explored here, the presence of glucose also affects the properties of the photoactivation process (see below) and the apparent initial distribution of S-states in dark-adapted samples (unpublished observations). The loss of activity in ΔpsbO cells is suppressed simply by incubating the cells at light intensities that are subsaturating for H_2O-splitting activity (5−30 μEinsteins m^{-2} s^{-1}). Incubation at substantially higher light intensities leads to irreversible losses due to the enhanced sensitivity to photoinhibition exhibited by *psbO*$^-$ strains (Mayes et al., 1991). In contrast to the dark losses in the mutant, wild-type cells typically lose little (<10%) activity even after 6 h in the dark (not shown). Earlier studies of photoactivation in cyanobacteria by Cheniae and

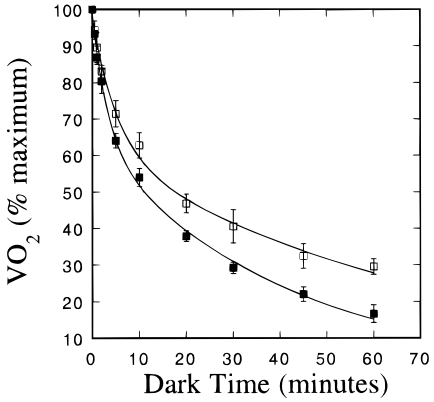

FIGURE 1: Dark decay of oxygen evolution activity in the MSP-less mutant, ΔpsbO. Autotrophically grown cells were harvested in late log phase, resuspended to a density corresponding to 200 μg of Chl/mL, allowed to equilibrate with shaking in the low light to achieve maximal activity, and placed in the dark with shaking in HN buffer (Materials and Methods) in the presence (solid squares) and absence (empty squares) of 5 mM glucose. Averages of three separate experiments are shown with error bars indicating standard deviations. Average (n = 3) maximal rate of DCBQ-supported O_2 evolution (VO_2) prior to transfer to the darkness was 178 ± 18 SD μmol of O_2 (mg of Chl)$^{-1}$ h^{-1} and represents 100% on the *y*-axis. The curves represent best fits of the data and consist of the sum of two exponential decay components which had half-times of 3.7 and 52 min for the minus glucose treatment and 2.3 and 28.9 min for the plus glucose treatment.

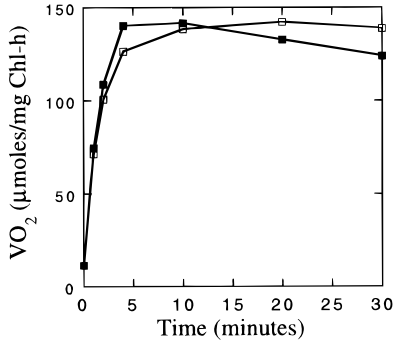

FIGURE 2: Photoactivation of dark-deactivated mutant cells under continuous illumination at two different light intensities: 15 (empty squares) and 65 (solid squares) μmol of photons m^{-2} s^{-1}. Cells that had been dark-deactivated in HN buffer (Materials and Methods) by 6 h of dark treatment were returned to the light for determination of DCBQ-supported O_2 evolution (VO_2) obtained upon photoactivation at various time intervals following the onset of illumination. The initial activity of cells prior to dark deactivation was measured to be 155 μmol of O_2 (mg of Chl)$^{-1}$ h^{-1}.

Martin (1972) demonstrated that changes in light-saturated rates of oxygen evolution reflect changes in the number of active PSII centers under experimental conditions similar to those employed here. The presence of DCBQ as the artificial electron acceptor eliminates the possibility that the reactivation observed here is due to a relief of acceptor-side limitation. On the basis of these considerations, we conclude that maximal activity is proportional to the concentration of oxygen-evolving PSII centers and the loss of activity corresponds to the progressive loss in the number of active PSII centers during dark incubation.

Reversal of lost activity in dark-deactivated mutant cells could be observed by returning deactivated samples to continuous illumination. Figure 2 shows deactivated samples (6 h darkness) returned to relatively low light fluences (15 μEinsteins m^{-2} s^{-1}) exhibit a fast recovery of activity that is essential complete within 10 min. The apparent rate of

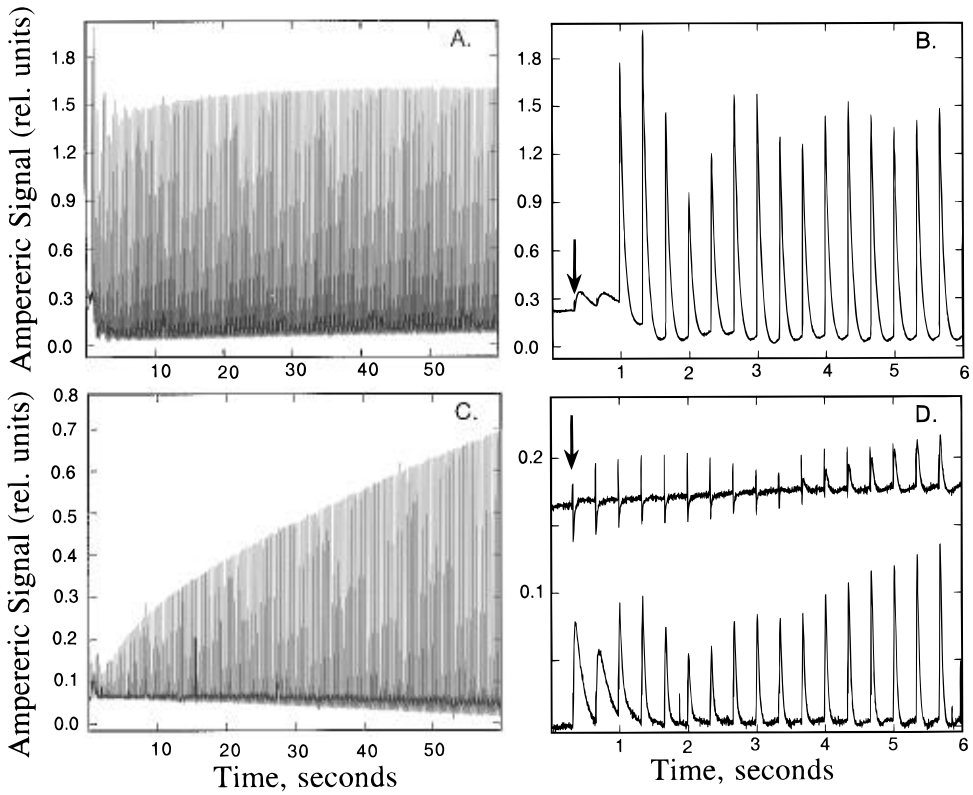

FIGURE 3: Photoactivation of dark-incubated wild-type (A and B) cells and mutant cells (C and D) by flash excitation on a bare platinum electrode. Wild-type (A and B) and ΔpsbO (C and D) were placed in darkness with for 4 h in HN buffer (Materials and Methods), except for the sample corresponding to the upper trace in panel D, which was placed in the dark for 36 h. Following dark treatment, cells were centrifugally deposited on a bare platinum electrode in the dark and subjected to a sequence of 179 flashes given at 3 Hz. The entire 60 s data acquisition for each sample is shown on the left (panels A and C). The first 6 s (17 flashes) of the same traces are shown in expanded form on the right (panels B and D). For wild-type cells (panel B), the relative concentrations of the S-states, including super-reduced states S_{-1} and S_{-2} , were estimated (Meunier et al., 1995b) to be $S_{-2} = 4\%$, $S_{-1} = 22.3\%$, $S_0 = 37.4\%$, $S_1 = 36.3\%$, $S_2 = 0\%$, and $S_3 = 0\%$. A similar analysis of the ΔpsbO flash pattern was not possible because of the large relative contribution to the positive deflection of the ampermeric signal from inhibition of respiration (Meunier et al., 1995a).

photoactivation was not discernibly increased by illumination at greater light intensities (60 μEinsteins m^{-2} s^{-1}), indicating saturation of the photoactivation process at low light fluences. In comparison, maximal rates of H_2O splitting in *Synechocystis* typically saturate in the range of 400−600 μEinsteins m^{-2} s^{-1} for cells grown under our culture conditions.

Dark losses and light-dependent restoration of activity in ΔpsbO cells were also observed during the course of routine experiments measuring flash O_2 yield using a bare platinum electrode. The flash O_2 yields of mutant cells partially deactivated on the unpolarized electrode could be reversed under a train of measuring flashes (not shown, but see below). Although it was possible to deactivate wild-type cells by very prolonged incubation on a polarized bare platinum electrode, we never observed any significant photoactivation during the ensuing flash sequence (not shown). To explore the flash photoactivation phenomenon in the mutant further and to minimize potential artifacts associated with prolonged incubation on the electrode, ΔpsbO cells were dark-deactivated for 4 h in a flask before flash O_2 yield measurements. Samples were then deposited on the electrode, and the ampermeric signal was recorded during a train of 179 flashes given at 3 Hz. Oxygen production transients are initially small and increase dramatically during the flash sequence (Figure 3C). After the total of 179 flashes shown in Figure 3C, the O_2 signal height reaches about 70% the maximal signal height seen after additional flashing (not shown). A similar extent of photoactivation was obtained with the mutant after extending the dark deactivation period to 36 h (data not shown). In contrast to MSP-less cells, there is no evidence for gradually increasing signal amplitudes from wild-type cells incubated in the dark (Figure 3A). Only the normal period four oscillations associated with the cycling of the S-states can be seen in the initial portion of the wild-type trace, as better seen in expanded form shown in Figure 3B. Note that the maximal O_2 yield is shifted from the third flash yield (typically seen after 10 min dark-adaptation) to the fourth flash. This indicates the accumulation of so-called super-reduced S-states, S_{-1} and S_{-2} (Bouges-Bocquet, 1973, Messinger & Renger, 1993). Mathematical deconvolution of the O_2 yield pattern (Meunier et al., 1995b) indicates rather normal miss and double-hit parameters (not shown), and an initial population of centers in the S_{-1} and S_{-2} states as 22% and 4%, respectively (see Figure 3 legend also). The small, more slowly rising signals (peaking at about 60 ms post-flash) after the first and second flash are seen in cyanobacterial samples and are not attributable to PSII activity, but reflect light-dependent inhibition of respiratory O_2 uptake [i.e., Kok effect (Myers & Graham, 1983; Meunier et al., 1995a)].

The corresponding expansion of the initial portion of the deletion mutant trace is shown in Figure 3D (lower trace, note vertical scale difference). Again small slowly rising signals are observed after the first and second flashes, followed by small transients attributable to PSII O_2 production. Clearly, some, albeit a small minority, of the PSII

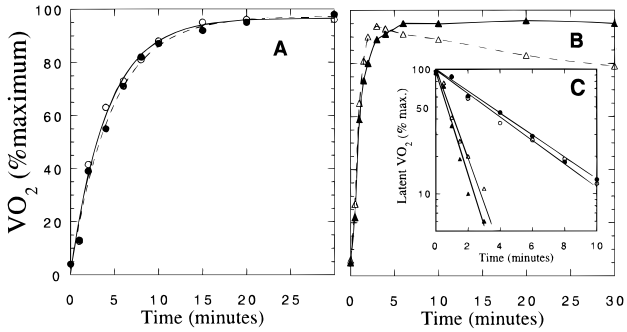

FIGURE 4: Photoactivation of hydroxylamine (HA)-extracted wild-type (panel A, open and closed circles) and ΔpsbO cells (panel B, open and closed triangles) exposed to continuous illumination at two different light intensities: 15 (open symbols) and 65 (solid symbols) μmol of photons m^{-2} s^{-1}. Panel C plots the decline in the percent of unphotoactivated ("Latent") PSII centers during the initial course of the photoactivation treatment, with symbols according to panels A and B. HA-extracted cells exhibited VO_2 values of 22 (wild-type) and 14 (ΔpsbO) μmol of O_2 (mg of Chl)$^{-1}$ h^{-1} prior to photoactivation treatments. Maximum rates (100%) of the VO_2 were obtained upon photoactivation of HA-extracted samples under low light conditions (see Materials and Methods) and were 418 (wild-type) and 163 (ΔpsbO) μmol of O_2 (mg of Chl)$^{-1}$ h^{-1}, whereas the corresponding preextracted rates were 489 (wild-type) and 189 (ΔpsbO) μmol of O_2 (mg of Chl)$^{-1}$ h^{-1}.

centers remain active even after 4 h of dark. However, a 36 h dark incubation results in a complete loss of activity in the mutant (Figure 3D, upper trace), although little loss of activity was observed for the wild-type kept under similar conditions (not shown). Under these conditions, the cellular respiratory reserves are depleted, and the slower transients are eliminated, allowing better resolution of the initial development of oxygen-evolving capacity during the flash sequence. The slowly rising signals are absent under these conditions (Meunier et al., 1995a), and O_2 is first discernible after the tenth or eleventh flash.

We next compared photoactivation of ΔpsbO and wild-type cells using samples pretreated with 1 mM hydroxylamine (HA) for 10 min to extract active site Mn from PSII. Previous work with intact cyanobacterial cells utilized a similar HA extraction protocol and established the basic kinetic mechanism of photoactivation, the "two-quantum model" (see Scheme 1 and Discussion). As with the photoactivation of HA-treated *Synechococcus* cells (Cheniae & Martin, 1972a) and similar to the photoactivation of dark-deactivated ΔpsbO cells, photoactivation of HA-treated wild-type and ΔpsbO cells required relatively low light intensities. Virtually identical photoactivation kinetics were observed for the wild-type at light intensities of 15 and 60 μEinsteins m^{-2} s^{-1}, and an analogous situation was observed for the mutant (Figure 4). Photoactivation at lower light intensities was optimal, especially for the mutant, since photoinhibitory effects were less pronounced. This is consistent with findings that ΔpsbO is especially prone to photoinhibition (Mayes et al., 1991), presumably due to reduced efficiency of electron transfer on the donor side of the PSII reaction center (Burnap et al., 1992; Mayes et al., 1991; Philbrick et al., 1991). Remarkably, the rate of photoactivation proved to be much higher for the mutant (Figure 4B) than the identically treated wild-type (Figure 4A). The rate of photoactivation in the different samples can be best compared by plotting the logarithm of latent activity against time (Figure 4C). Linearity of these plots indicates the photoactivation rate is proportional to the number of un-reactivated

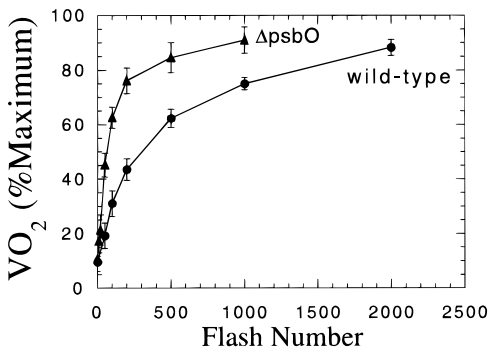

FIGURE 5: Photoactivation of HA-extracted wild-type cells (circles) and ΔpsbO cells (triangles) as a function of flash number. HA-extracted cells in HN buffer with 5 mM glucose were subjected various numbers of flashes given at 2 Hz. HA-extracted cells had VO_2 values of 22 (wild-type) and 14 (ΔpsbO) μmol of O_2 (mg of Chl)$^{-1}$ h^{-1} prior to photoactivation treatments. Data points represent the averages of 3−5 experiments, and error bars signify 1 SD.

centers present in the sample and the magnitude of the negative slope is proportional to the rate of photoactivation (Cheniae & Martin, 1972a; Tamura & Cheniae, 1987). Neglecting deviations from linearity at later time points due to irreversible losses from photoinhibition, this analysis shows the rate of photoactivation in the mutant is approximately 4-fold faster than in the wild-type: half-times ($t_{1/2}$) of 3.5 and 0.8 min for the rate of photoactivation were obtained for wild-type and ΔpsbO cells, respectively. For comparison, half-times of 3.2 and 6 min were previously obtained for the photoactivation of HA-extracted wild-type *Synechococcus* cells and HA-extracted PSII membranes (Tamura & Cheniae, 1987).

Single-turnover flash photoactivation measurements were performed to determine possible differences in the relative quantum of photoactivation of the mutant and wild-type. Figure 5 plots photoactivation as a function of flash number. Greater than 50% of the latent activity in the mutant is restored within the first 70−80 flashes, whereas similar restoration takes greater than 300 flashes in the wild-type, indicating that the MSP-less strain has an approximately 4-fold greater overall quantum yield of photoactivation than the wild-type. The comparatively low quantum yields for the wild-type are typical of the photoactivation process, and the results obtained here with the wild-type are comparable to the results obtained from flash photoactivation of HA-extracted wild-type *Synechococcus* cells (Cheniae & Martin, 1972a).

Figure 6 shows the extent of photoactivation resulting from 100 flashes given at different flash intervals. This type of analysis provides information on the kinetics of the rate-limiting steps and the lifetimes of unstable intermediate photoproducts of the multiquantum photoactivation process (see Discussion and Scheme 1). Both the wild-type and mutant exhibit the characteristic bell-shaped curve observed previously *in vivo* (Cheniae & Martin, 1972a,b) and *in vitro* (Miyao & Inoue, 1991; Tamura & Cheniae, 1987); however, in contrast to the wild-type, significant yields are observed in the mutant even at the highest flash frequencies permitted by our instrumentation. The flash interval-dependent yields shown in Figure 6 demonstrate that photoactivation in *Synechocystis* conforms to the previously established mechanism. It therefore provides circumstantial evidence that the HA treatment used here removes all PSII active site Mn

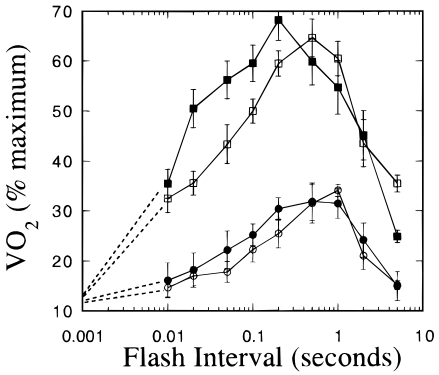

FIGURE 6: Photoactivation of HA-extracted wild-type cells (circles) and mutant cells (squares) under flash illumination given at different intervals. HA extracted in HN buffer with 5 mM glucose (closed symbols) and without glucose (open symbols) were subjected to 100 flashes, and the rate of light-saturated DCBQ-supported O_2 evolution was determined. The dashed lines are drawn to indicate the level of activity prior to flash photoactivation and are about 10−12% of the preextracted activity for all sample types. Data points represent the averages of 3−6 experiments, and error bars signify 1 SD. Maximum rates (100%) refer to O_2 evolution rates obtained upon photoactivation of HA-extracted samples under low light conditions (see Materials and Methods) and were 423 (wild-type) and 169 (ΔpsbO) μmol of O_2 (mg of Chl)$^{-1}$ h^{-1}, whereas the corresponding preextracted rates were 493 (wild-type) and 178 (ΔpsbO) μmol of O_2 (mg of Chl)$^{-1}$ h^{-1}.

removed in previous photoactivation studies. Consistent with previous reports, low yields of assembled centers are obtained in the wild-type when the spacing of flashes is very short (Δt < 50 ms). This phenomenon reflects the existence of a low quantum yield process initiating a dark step(s) that must go to completion before effective utilization of the next quantum occurs (see Scheme 1). The fact that comparatively high yields are obtained in the mutant even at the shortest flash intervals is consistent with the higher relative quantum yields seen in Figure 5 and suggests that centers are more efficiently initiated or stabilized by some light-dependent step along the assembly pathway. Low yields seen in all samples at long flash intervals (Figure 6) also reflect the multiquantum requirement of photoactivation, since it is expected that the product of the first quantum absorbed by the center has a greater probability of decaying if a second quantum arrives at a long interval after the first. The slope of the descending portion provides an estimate of the lifetime of the unstable intermediate, whereas the slope of the ascending portion of the curve is related to the rate constant of this (these) dark step(s). The half-time of the dark rearrangement and the half-lifetime of the unstable intermediate are estimated to be approximately 140 ms and about 4 s, respectively, for wild-type samples in the presence of glucose and 150 ms and about 3 s, respectively, for wild-type samples in the absence of glucose. The mutant sample without glucose exhibits an approximately 100 ms half-time for the dark step, estimating from the ascending region of the graph, although it is clear that a faster additional component remains unresolved. The ascending portion of the graph is more complex in the mutant in the presence of glucose, making evaluation of dark rearrangement more difficult. The half-lifetimes of the unstable intermediate in the mutant samples are estimated to be approximately 1 s in the presence of glucose and about 2 s in the absence of glucose.

DISCUSSION

The data presented here show that genetic removal of MSP results in a large decrease in the dark stability of PSII O_2 evolution activity and, more surprisingly, results in a pronounced increase in the apparent quantum yield of photoactivation. The fact that O_2 evolution activity declines precipitously in the dark in the absence of MSP is consistent with previous *in vitro* studies showing that MSP stabilizes the binding of PSII Mn. Those studies demonstrated the Cl^--sensitive loss of two of the four active site Mn atoms in spinach PSII membranes. The present observations are also consistent with recent reports describing the decay in oxygen evolution activity in MSP-less cyanobacteria (*Synechocystis* and *Synechococcus*) (Engels et al., 1994) and the characterization of a *Synechocystis* strain having short deletions in the lumenal E loop of the CP47 causing impaired MSP binding (Gleiter et al., 1994, 1995). Because maintaining samples in the light prevents losses in O_2 evolution, it is likely that deactivation involves the formation of unstable reduced intermediates of the Mn tetramer (Cheniae & Martin, 1971; Yocum et al., 1981) and that generation of photooxidant at the reaction center counteracts the reduction and concomitant destabilization of the Mn cluster. The acceleration of PSII deactivation by glucose (Figure 1), a source of metabolic reductant, is consistent with this idea as is the shortening of the lifetime of the second unstable photoactivation intermediate and the concomitant shifting of the optimum to shorter flash intervals in the presence of glucose shown in Figure 6. The results of recent fluorescence yield measurements of *Synechocystis* cells (Chu et al., 1994b) also provide evidence for the existence of an endogenous reductant(s) capable of interacting with the donor side of PSII. These data suggest loss of Mn from the active site is mediated by an endogenous reductant. They do not, however, discriminate between the loss of one or two labile Mn or the entire set of four Mn of the cluster in dark-deactivated cells since each alternative would result in the loss of O_2 evolution.

The existence of an endogenous reductant also best explains the accumulation of apparent S_{-1} and S_{-2} states observed after prolonged dark incubation of the wild-type (Figure 3 and its legend). Studies on the reaction of exogenous reductants (e.g., 50 μM hydroxylamine) with the Mn cluster in isolated PSII particles and PSII membranes have identified the S_{-1} and S_{-2} states as super-reduced forms of the Mn tetramer. A plausible mechanism for the dark loss of activity might thus involve reduction of active site Mn in its "normal" higher oxidation states to form Mn^{2+}, which would be prone to dissociate from the H_2O oxidation complex, especially in the absence of MSP. Similar conclusions were reached upon analysis of certain CP47 mutants that have short deletions in the large lumenal "E" loop and are also prone to dark deactivation (Gleiter et al., 1995). On this basis, we propose that an important function of MSP is to stabilize the Mn cluster in a metastable condition during episodes of darkness when super-reduced states of the cluster are populated due to the action of endogenous reductants. Destruction of the active site Mn tetramer by exogenous reductants is already well documented and shows that the extrinsic polypeptides and Ca^{2+} each protect the Mn cluster. Mei and Yocum (1991) characterized a calcium-sensitive intermediate of the reductive inactivation process having Mn

Scheme 1

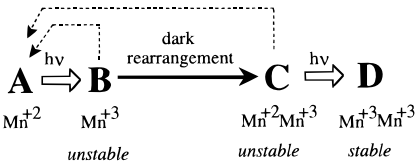

closely associated with the active site, but exhibiting the hexaquo EPR signal characteristic of solublized Mn^{2+}. Such a metastable state was persistent only in the presence of Ca^{2+}. Since MSP modulates the Ca^{2+} site of PSII, one possibility is that MSP stabilizes Ca^{2+} at the Mn cluster and in the absence of MSP Ca dissociates, rendering the Mn cluster either prone to attack by endogenous reductant and/or more prone to dissociate from the reaction center upon reduction.

The most interesting finding of this study was that the loss of MSP enhances the overall quantum efficiency of photoactivation. The rapid photoactivation of dark-deactivated PSII in cells lacking MSP (Figures 2 and 3) prompted us to examine photoactivation of HA-treated whole cells to directly compare the kinetics of photoactivation of the mutant and wild-type enzymes (Figures 4−6). An HA extraction protocol that is similar to the one employed here was developed previously with intact *Synechococcus* cells to extract active site Mn (Cheniae & Martin, 1972a). These and parallel pioneering studies established the basic kinetic features of the photoactivation process including the multiquantum requirement (see below). Subsequent *in vitro* studies using HA extraction procedures (Miller & Brudvig, 1989, 1990; Miyao & Inoue, 1991; Miyao-Tokutomi & Inoue, 1992; Tamura & Cheniae, 1986, 1987; Tamura et al., 1989) have confirmed the "two-quantum model" and implicate the photooxidation of two Mn^{2+} coupled to their assembly into the apoenzyme. Although it is well established that photoactivation of HA-treated samples may proceed in the absence of MSP (Miyao & Inoue, 1991; Tamura & Cheniae, 1986, 1987), a comparison of the kinetics ±MSP has not been performed. Photoactivation has a roughly 4-fold higher rate in the mutant compared to the wild-type under continuous illumination (Figure 4), and the mutant exhibits a correspondingly greater overall quantum efficiency of photoactivation as shown using single-turnover flash illumination (Figure 5). Photoactivation is postulated to be a multiquantum process involving the existence of two unstable intermediates separated by a light-independent (dark) rearrangement step, typically with a 150 ms half-time (Cheniae & Martin, 1972a,b; Tamura & Cheniae, 1987). This kinetic model, termed the "two-quantum series model", is summarized in Scheme 1 with corresponding hypothetical configurations of bound Mn added to facilitate discussion.

The so-called "rate-limiting" dark rearrangement is the conversion of first photoproduct **B** to intermediate **C**. Both **B** and **C** are unstable, with **C** being less stable and more susceptible to attack by exogenous reductants than **B** (Ono & Inoue, 1987). The first stable intermediate coincides with the formation of intermediate **D**, which then undergoes further conversions to form the active complex. This kinetic scheme accounts for the observation that photoactivation under a train of flashing light occurs with maximum yield at an optimum flash frequency as evidenced by all curves in Figure 6. Flashes given at intervals exceeding the lifetime of **C** tend to produce lower yields of active centers due to the decay of this unstable intermediate (seconds time range). In opposition, flashes given at intervals that are short compared to the apparent time constant of the dark rearrangement tend to give lower yields due to insufficient time for the requisite conversion (**B** → **C**) to occur prior to the subsequent flash. In this context, it is worth noting the distinction between the "rate-limiting" **B** → **C** rearrangement of PSII centers and the factors limiting the overall rate of photoactivation of a *population* of PSII centers. The **B** → **C** dark rearrangement limits the rate that an *individual* PSII center that has already entered the pathway advances further, whereas the photoactivation rate of a population of PSII centers *also* depends upon such things as the steady-state concentration of **B** formed and the rates of decay and photochemical stabilization of state **C**. In Figure 6, the entire Bell-shaped curve describing photoactivation of the mutant as a function of flash interval is shifted upward relative to the wild-type. This occurs in the absence of dramatic changes in the apparent rates of formation and decay of the intermediate, **C**, at least in the case of the minus-glucose sample as indicated by only a modest increase in the rising and falling slopes, respectively, of the curve in Figure 6. Significantly, moderate levels of photoactivation in the mutant were observed at the shortest flash intervals permitted by our instrument, in contrast to the wild-type, which showed virtually no photoactivation at these short intervals. This suggests that a process distinct from the light-independent **B** → **C** rearrangement is more efficient in the absence of MSP in accordance with the higher quantum yield observed in the mutant. This could be due to two general possibilities: *(case 1)* the absence of MSP results in a larger fraction of centers initiating the **B** → **C** rearrangement following the initial photoact (**A** → **B**); or *(case 2)* a larger fraction of centers that have completed the **B** → **C** rearrangement become photochemically stabilized (**C** → **D**) rather than decaying. Both possibilities correspond to increased quantum yields, but in *case 1* the higher yield is due to a higher quantum yield of **C** from **A** by the first quantum, whereas in *case 2* the higher quantum yield is due to a higher probability that the second quantum converts **C** to the first stable intermediate **D**.

The initial stage (**A** → **B**) of photoactivation involves the photooxidation of Mn^{2+} bound to the apoenzyme to form an unstable mononuclear Mn^{3+} intermediate (Miller & Brudvig, 1990). This may be followed by the binding of a second Mn^{2+} to form the binuclear $Mn^{3+}-Mn^{+2}$ intermediate, which must rearrange (**B** → **C**) before photooxidation of the second Mn occurs to form the relatively stable $Mn^{3+}-Mn^{3+}$ intermediate (**D**). Alternatively, the dark rearrangement (**B** → **C**) occurs prior to the binding of the second Mn^{2+}, which, upon binding, is photooxidized to form **D**. Oxidation of Mn^{2+} by Y_Z^+ during the first step of photoactivation occurs with a low quantum efficiency (Miller & Brudvig, 1990), whereas the quantum efficiency of oxidation of the second Mn^{2+} is less understood. In any event, the low yield of photoactivation is probably due to the competition between the charge recombination of $P680^+Q_A^-$ and the forward reactions involving oxidation of Mn^{2+} (Miller & Brudvig, 1989, 1990; Miyao-Tokutomi & Inoue, 1992; Tamura & Cheniae, 1987). Improvement in the quantum yield of *in vitro* photoactivation is correlated with the efficient reoxidation of Q_A^- by efficient artificial PSII electron acceptors (Miyao-Tokutomi & Inoue, 1992). Al-

though there are indications that the absence of MSP may cause changes on the acceptor side of PSII (Burnap & Sherman, 1991; Mayes et al., 1991), it seems likely that the major cause of the 4-fold boost in overall quantum efficiency of photoactivation upon deletion of MSP is a change on the donor side of PSII that increases the probability that $P680^+$ is used to oxidize Mn^{2+} instead of recombining with Q_A^-. One reasonable explanation for the increased efficiency of photoactivation in the mutant is the increased accessibility or binding affinity of Mn^{2+} to the active site and Y_Z^+. This would lead to a higher frequency of occupation of the Mn site and consequently a higher quantum yield due to the higher probability that photochemical oxidant from the reaction center would be utilized at this site for Mn^{2+} oxidation. According to this interpretation, the absence of MSP allows more efficient Mn^{2+}-mediated reduction of Y_Z^+, and since Y_Z^+ is in equilibrium with $P680^+$, this would result in a lower concentration of $P680^+$ after the flash and thus fewer back-reactions with Q_A^- (i.e., oxidation of Mn^{2+} via Y_Z more effectively competes with back -reactions). The absence of MSP therefore causes one or both of the two Mn^{2+} photooxidation steps of photoactivation to occur with higher quantum yield.

A more efficient oxidation of Mn^{2+} by Y_Z^+ in the absence of MSP is consistent with the results of Chu et al. (1994) with *Synechocystis* PSII mutants, indicating greater occupancy of the binding site and/or efficiency of photooxidation of Mn^{2+} in the absence of MSP. As noted by Chu et al., photooxidation of Mn in the absence of MSP seems to run counter to the results of Hoganson et al. (1989), who observed little apparent kinetic difference in Mn^{2+} oxidation by Y_Z^+ in the presence and absence of MSP in spinach PSII membranes. To account for the apparent discrepancy with binding/photooxidation of Mn^{2+} in PSII membranes, Chu et al. note differences in experimental conditions as well as the fact that the intact cyanobacterial H_2O oxidation complex may be fundamentally different than that of higher plants with respect to polypeptide composition and ion dependencies. Notably, the samples in Hoganson et al. experiments were poised, in terms of redox and flash frequency conditions, to repeatedly observe photooxidation of the first incoming Mn^{2+}. Since the increased quantum yield observed in the our photoactivation experiments could be attributed to enhanced binding/photooxidation of either the first or the second Mn^{2+}, or both, a possible explanation of the discrepancy between the Hoganson et al. experiments and the present experiments is that the absence of MSP affects the photooxidation of the second Mn^{2+}, but not the first.

The most straightforward explanation for the increased quantum yield of photoactivation is that MSP forms a diffusional barrier that limits access of Mn^{2+} to the binding/photooxidation site(s) that limit the quantum yield of photoactivation. This is consistent with findings that the extrinsic polypeptides lower the reactivity of the Mn cluster toward exogenous reductants, suggesting that the extrinsic polypeptides reduce accessibility to the catalytic site. Alternatively, the binding of MSP modifies the conformational state of the intrinsic portion of the PSII complex in a way that influences either the accessibility of Mn to its site of ligation or the affinity of its binding. Obviously, other scenarios can be envisioned. For example, MSP may affect the occupancy of the Ca^{2+} site, which, in turn, regulates the accessibility of Mn to the binding site (Mei & Yocum, 1991). In this case, the loss of MSP destabilizes Ca^{2+} binding, thus giving Mn greater accessibility to its site of ligation.

It is interesting to compare the results of Gleiter et al. (1994, 1995), who investigated CP47 mutants with short deletions in the 190 amino acid "E-loop". This region of CP47 is proposed to be in close proximity to the H_2O oxidation domain of PSII (Bricker, 1990; Eaton-Rye & Vermaas, 1991; Haag et al., 1993) and provides a binding site for MSP (Bricker et al., 1988, Odom & Bricker, 1992). Certain of the short deletions in this region weaken binding of MSP [e.g., Δ(A373−D380)], and several mutants exhibit a dark-labile H_2O oxidation complex, although the rate of dark inactivation is at least several times slower than that observed for the ΔpsbO mutant. Interestingly, the Δ(A373−D380) and Δ(R384−V392) mutants exhibit similar rates of dark deactivation, and yet show very different flash yields of photoactivation. The Δ(A373−D380) mutant is maximally photoactivated within 200 flashes, which is similar to 200−300 flashes necessary to completely restore dark-deactivated ΔpsbO cells (Figure 3). In contrast to the relatively efficient photoactivation of Δ(A373−D380) and ΔpsbO, the Δ(R384−V392) mutant requires over 2000 flashes to achieve maximal photoactivation. This is similar to the number of flashes required to photoactivate HA-extracted wild-type cells (Figure 5). Despite the differences between the Δ(A373−D380) and Δ(R384−V392) mutants, photoactivation in both strains is dramatically stimulated by the addition of 10 mM $CaCl_2$ to dark-deactivated cells before giving photoactivating flashes. A similar $CaCl_2$ effect in the ΔpsbO mutant is not observed despite repetitive efforts. This is curious since the ΔpsbO mutant requires higher levels of Ca^{2+} for autotropic growth than the CP47 mutants. Clarification of these various photoactivation phenotypes will require further experimental analysis.

Finally, it is worth noting that mutations increasing the efficiency of a vital biochemical process, in this case photoactivation, are probably rare. Evidently by maintaining the extrinsic polypeptides of the PSII complex, selective pressure has placed more value upon (1) optimization of the catalytic efficiency of the water-splitting process, (2) sequestration of the active site Mn to prevent destructive dissipation of accumulated charge, and (3) the dark stability of the enzyme, all this in preference to maximizing the rate at which PSII centers can be assembled.

ACKNOWLEDGMENT

We thank Dr. George Cheniae, Dr. Terry Bricker, and Dr. Rick Debus for valuable discussions and Dr. Pascal Meunier for providing the eigenvalue fitting and analysis algorithms. We also thank Dr. Bruce Diner for useful advice on the construction of the centrifugal electrode and Dr. Jack Myers for sending plans and giving advice for the construction of the turbidostats.

REFERENCES

Andersson, B., & Akerland, H.-E. (1987) *Top. Photosynth. 8*, 379−420.

Babcock, G. T., Barry, B. A., Debus, R. J., Hoganson, C. W., Atamian, M., McIntosh, L., Sitole, I., & Yocum, C. F. (1989) *Biochemistry 28*, 9557−9565.

Bouges-Bocquet, B. (1973) *Biochim. Biophys. Acta 292*, 772−785.

Bricker, T. M. (1990) *Photosynth. Res. 24*, 1−13.

Bricker, T. M. (1992) *Biochemistry 31*, 4623−4628.

Bricker, T. M., Odom, W. R., & Queirolo, C. B. (1988) *FEBS Lett. 231*, 111−117.
Burnap, R., & Sherman, L. A. (1991) *Biochemistry 30*, 440−446.
Burnap, R., Shen, J. R., Jursinic, P. A., Inoue, Y., & Sherman, L. A. (1992) *Biochemistry 31*, 7404−7410.
Burnap, R. L., Qian, M., Shen, J. R., Inoue, Y., & Sherman, L. A. (1994) *Biochemistry 33*, 13712−13718.
Cheniae, G. M., & Martin, I. F. (1971) *Plant Physiol. 47*, 568−575.
Cheniae, G. M., & Martin, I. F. (1972a) *Plant Physiol. 50*, 87−94.
Cheniae, G. M., & Martin, I. F. (1972b) *Biochim. Biophys. Acta 253*, 167−181.
Chu, H.-A., Nguyen, A. P., & Debus, R. A. (1994a) *Biochemistry 33*, 6150−6157.
Chu, H.-A., Nguyen, A. P., & Debus, R. A. (1994b) *Biochemistry 33*, 6137−6149.
Debus, R. J. (1992) *Biochim. Biophys. Acta 1102*, 269−352.
Eaton-Rye, J. J., & Vermaas, W. F. J. (1991) *Plant Mol. Biol. 17*, 1165−1178.
Engels, D. H., Lott, A., Schmid, G. H., & Pistorious, E. K. (1994) *Photosynth. Res. 42*, 227−244.
Ghanotakis, D. F., & Yocum, C. F. (1990) *Annu. Rev. Plant Physiol. Plant Mol. Biol. 41*, 255−276.
Gleiter, H. M., Haag, E., Shen, J. R., Eaton-Rye, J. J., Inoue, Y., Vermaas, W. F. J., & Renger, G. (1994) *Biochemistry 33*, 12063−12071.
Gleiter, H. M., Haag, E., Shen, J. R., Eaton-Rye, J. J., Seeliger, A. G., Inoue, Y., Vermaas, W. F. J., & Renger, G. (1995) *Biochemistry 34*, 6847−6856.
Haag, E., Eaton-Rye, J. J., Renger, G., & Vermaas, W. F. J. (1993) *Biochemistry 32*, 4444−4454.
Kuwabara, T., Miyao, M., Murata, T., & Murata, N. (1985) *Biochim. Biophys. Acta 806*, 283−289.
Mayes, S. R., Cook, K. M., Self, S. J., Zhang, Z., & Barber, J. (1991) *Biochim. Biophys. Acta 1060*, 1−12.
Mei, R., & Yocum, C. F. (1991) *Biochemistry 30*, 7863−7842.
Messinger, J., & Renger, G. (1993) *Biochemistry 32*, 9379−9386.
Meunier, P. C., & Popovic, R. (1988) *Rev. Sci. Instrum. 59*, 486−491.
Meunier, P. C., Burnap, R. L., & Sherman, L. A. (1995a) *Photosynth . Res. 45*, 31−40.
Meunier, P. C., Burnap, R. L., & Sherman, L. A. (1995b) *Photosynth. Res.* (in press).
Miller, A.-F., & Brudvig, G. W. (1989) *Biochemistry 28*, 8181−8190.
Miller, A.-F., & Brudvig, G. W. (1990) *Biochemistry 29*, 1385−1392.
Miyao, M., & Inoue, I. (1991) *Biochemistry 30*, 5379−5287.
Miyao-Tokutomi, M., & Inoue, Y. (1992) *Biochemistry 31*, 526−532.
Miyao, M., Murata, N., Lavorel, J., Maison-Peteri, B., Boussac, A., & Etienne, A.-L. (1987) *Biochim. Biophys. Acta 890*, 151−159.
Myers, J., & Graham, J. R. (1983) *Biochim. Biophys. Acta 722*, 281−290.
Odom, W., & Bricker, T. M. (1992) *Biochemistry 31*, 5616−5620.
Ono, T. A., & Inoue, Y. (1982) *Plant Physiol. 69*, 1418−1422.
Ono, T. A., & Inoue, Y. (1987) *Plant Cell Physiol. 28*, 1293−1300.
Philbrick, J. B., Diner, B. A., & Zilinskas, B. A. (1991) *J. Biol. Chem. 266*, 13370−13376.
Tamura, N., & Cheniae, G. M. (1986) *FEBS Lett. 200*, 231−236.
Tamura, N., & Cheniae, G. (1987) *Biochim. Biophys. Acta 890*, 179−194.
Tamura, N., Inoue, Y., & Cheniae, G. (1989) *Biochim. Biophys. Acta 976*, 173−181.
Tamura, N., Inoue, H., & Inoue, Y. (1990) *Plant Cell Physiol. 31*, 469−477.
Vass, I., Ono, T. A., & Inoue, Y. (1987) *FEBS Lett. 211*, 215−220.
Williams, J. G. K. (1988) *Methods Enzymol. 167*, 766−778.
Yocum, C. F., Yerkes, C. T., Blankenship, R. E., Sharp, R. R., & Babcock, G. T. (1981) *Proc. Natl. Acad. Sci. U.S.A. 78*, 7507−7511.

BI951964J